The Stalk Domain and the Glycosylation Status of the Activating Natural Killer Cell Receptor NKp30 Are Important for Ligand Binding*[S]

Jessica Hartmann[‡], Thuy-Van Tran[‡], Janina Kaudeer[‡], Karin Oberle[§], Julia Herrmann[‡], Isabell Quagliano[‡], Tobias Abel[¶], André Cohnen[||], Volker Gatterdam[**], Andrea Jacobs[‡‡], Bernd Wollscheid[‡‡], Robert Tampé[**], Carsten Watzl[||], Andreas Diefenbach[§], and Joachim Koch[‡1]

From the [‡]Georg-Speyer-Haus, Institute of Biomedical Research, D-60596 Frankfurt am Main, Germany, [§]Institute of Medical Microbiology and Hygiene, University of Freiburg Medical Center, D-79106 Freiburg, Germany, [¶]Paul-Ehrlich-Institut, Division of Medical Biotechnology, D-63225 Langen, Germany, [||]Leibniz Research Centre for Working Environment and Human Factors (IfADo), D-44139 Dortmund, Germany, [**]Institute of Biochemistry, Biocenter, Goethe University, D-60438 Frankfurt am Main, Germany, and [‡‡]Eidgenössische Technische Hochschule (ETH) Zürich, Institute of Molecular Systems Biology, CH-8093 Zürich, Switzerland

Background: NKp30 is a major activating receptor of natural killer (NK) cells.
Results: The stalk domain of NKp30 increases ligand binding affinity, which is modulated by glycosylation of the ectodomain of NKp30.
Conclusion: The stalk domain and the glycosylation status of NKp30 are critical for NK cell killing.
Significance: This is the first hint for a novel mode of receptor regulation.

The natural cytotoxicity receptors are a unique set of activating proteins expressed mainly on the surface of natural killer (NK) cells. The human natural cytotoxicity receptor family comprises the three type I membrane proteins NKp30, NKp44, and NKp46. Especially NKp30 is critical for the cytotoxicity of NK cells against different targets including tumor, virus-infected, and immature dendritic cells. Although the crystal structure of NKp30 was recently solved (Li, Y., Wang, Q., and Mariuzza, R. A. (2011) *J. Exp. Med.* 208, 703–714; Joyce, M. G., Tran, P., Zhuravleva, M. A., Jaw, J., Colonna, M., and Sun, P. D. (2011) *Proc. Natl. Acad. Sci. U.S.A.* 108, 6223–6228), a key question, how NKp30 recognizes several non-related ligands, remains unclear. Therefore, we investigated the parameters that impact ligand recognition of NKp30. Based on various NKp30-hIgG1-Fc fusion proteins, which were optimized for minimal background binding to cellular Fcγ receptors, we identified the flexible stalk region of NKp30 as an important but so far neglected module for ligand recognition and related signaling of the corresponding full-length receptor proteins. Moreover, we found that the ectodomain of NKp30 is N-linked glycosylated at three different sites. Mutational analyses revealed differential binding affinities and signaling capacities of mono-, di-, or triglycosylated NKp30, suggesting that the degree of glycosylation could provide a switch to modulate the ligand binding properties of NKp30 and NK cell cytotoxicity.

Natural killer (NK)[2] cells are large granular lymphocytes of the innate immune system that spontaneously kill foreign, tumor, and virus-infected cells (1–3). Additionally, NK cells act as immune regulators by secretion of chemokines and cytokines and/or by direct interaction with other immune cells such as dendritic cells (DCs) (4, 5). The impact of NK cells for immunosurveillance of virus-infected and tumor cells becomes evident when NK cell cytotoxicity is limited by efficient immune escape strategies used by these cells, consequently leading to disease (2).

NK cells are tightly regulated by a dynamic balance of signals from several agonistic and antagonistic cell surface receptors to prevent destruction of healthy cells while maintaining recognition and efficient killing of multiple adverse targets (1, 6). NK activating receptors recognize viral and frequently induced cellular ligands, whereas most inhibitory receptors recognize self-major histocompatibility class I (MHC I) molecules (7). The major activating receptors on human NK cells include NKG2D and the natural cytotoxicity receptors (NCRs) NKp30, NKp44, and NKp46 (7). The expression of an insufficient amount of NCRs results in resistance of leukemia cells to NK cell cytotoxicity in patients with acute myeloid leukemia (8), demonstrating their importance for immunosurveillance of tumor cells. Notably, NKp30 and NKp46 are found on all NK cells, whereas NKp44 represents a marker for activated NK cells (6, 9). The density of NCRs on the cell surface correlates with the degree of NK cell cytotoxicity against various tumors (10, 11). Interestingly, the ligands of NCRs are expressed in many tissues includ-

[2] The abbreviations used are: NK, natural killer; NCR, natural cytotoxicity receptor; DC, dendritic cell; TMD, transmembrane domain; BAG-6, BCL2-associated athanogene 6; LBD, ligand-binding domain; NF-AT, *nuclear factor of activated T cells*; SPR, surface plasmon resonance; PMA, phorbol 12-myristate 13-acetate; hIg, human immunoglobulin; FcγR, Fcγ receptor; RU, resonance units.

ing healthy cells and tumor cells (10); therefore, their expression level is critical for the ability of NK cells to destroy target cells (8, 12–15). The human cytomegalovirus (CMV) tegument protein pp65 (16), the BCL2-associated athanogene 6 (BAG-6; also known as BAT3) (17, 18), and a structural homolog of B7 (B7-H6) (19) were shown as ligands for NKp30, indicating ligand promiscuity of NKp30. Although ligation of pp65 leads to inhibition of NK cell cytotoxicity as part of an immune escape strategy (16), engagement of BAG-6 or B7-H6 on tumor cells mediates target cell killing (17, 19). Moreover, binding of NKp30 to BAG-6 on DCs leads to DC activation and killing of immature tolerogenic DCs as part of a quality control mechanism (18, 20, 21). Controversial data exist for potential binding of NKp30 to heparan sulfate/heparin molecules (22, 23). NKp30, NKp44, and NKp46 recognize viral hemagglutinins (HAs) (24–27), and binding of HA to NKp44 and NKp46 consequently promotes NK cell killing of virus-infected cells (24–27). Recently, the proliferating cell nuclear antigen was discovered as a novel inhibitory ligand for NKp44 (28).

NKp30 comprises an extracellular ligand binding domain, a transmembrane domain (TMD) that recruits the signaling adaptor protein CD3ζ, and a short cytoplasmic tail (6, 12). The N-terminal part of the ectodomain of NKp30 comprises an Ig-like fold (ligand-binding domain (LBD)) (29, 30), which is connected to the TMD by a flexible stalk domain.

In the current study, we identified the so far neglected stalk domain of NKp30 as an essential element for ligand binding. Moreover, we demonstrate that NKp30 is *N*-linked glycosylated at three consensus sequence motifs. Detailed studies revealed that differential glycosylation impacts the ligand binding properties of NKp30 and might be a switch to modulate NK cell cytotoxicity.

EXPERIMENTAL PROCEDURES

Antibodies—For Western blotting, the following antibodies were used: anti-human NKp30, polyclonal (AF1849, R&D Systems); anti-goat IgG (HRP conjugate; A5420, Sigma-Aldrich); and anti-human IgG-Fc (HRP conjugate; A0170, Sigma-Aldrich). For immunofluorescence microscopy and flow cytometry, the following antibodies were used: anti-human NKp30, clone P30-15 (allophycocyanin conjugate; 325209, BioLegend); anti-mouse CD4, clone RM4-5 (allophycocyanin conjugate; 17-0042, eBioscience); anti-human IgG-Fc (DyLight 488 conjugate; 109-485-008, Dianova); and anti-human IgG-Fc (DyLight 649 conjugate; 109-495-008, Dianova).

Cells—Human chronic myeloid leukemia cells (K-562, CCL-243), human embryonic kidney cells (293, CRL-1573; 293T/17, CRL-11268), African green monkey kidney cells (COS-7, CRL-1651), and Chinese hamster ovarian cells (CHO K1, CCL-61) were purchased from American Type Culture Collection (ATCC). Murine pro-B cells (Ba/F3, ACC 300) were purchased from Deutsche Sammlung von Mikroorganismen und Zellkulturen (DSMZ). Human melanoma cells (MelJuSo) were kindly provided by E. Wiertz (31). Ba/F3 cells transduced with B7-H6 (Ba/F3-B7-H6) or the empty vector (Ba/F3-mock) were provided by C. Watzel (IfADo, Germany), and A5 cells were kindly provided by A. Diefenbach (32).

Recombinant Ig Proteins—To generate NKp30-Ig fusion proteins, the pFUSE-hIgG1-Fc2 vector (InvivoGen) was used. Two single (L118E (E) and N180Q (Q)) and one double mutation (L118E/N180Q (EQ); amino acid positions refer to UniProtKB/Swiss-Prot accession number P01857) were introduced into the hIgG1-Fc part by site-directed mutagenesis. To generate 30LBD-Ig, 30Stalk-Ig, and Ifnar2-Ig fusion proteins, the ectodomain-encoding gene segment of NKp30 (NCBI RefSeq accession number NM_147130.2; 30LBD-Ig, residues 19–128; 30Stalk-Ig, residues 19–143) and Ifnar2 (GenBank™ accession number X89814.1; Ifnar2-Ig, residues 28–239) were amplified by PCR from cDNA (NKp30 (GenScript); the Ifnar2 DNA was kindly provided by J. Piehler (University of Osnabrück, Germany)) and cloned into pFUSE-hIgG1-Fc2 vector variants. The pFUSE-hIgG1-FcEQ vector with a 30Stalk insert was used as template to produce an NKp30-Ig fusion construct containing a length-matched glycine-serine (GS) linker instead of the stalk domain (30GS-Ig) and three C-terminally truncated 30Stalk-Ig variants (30Stalk-Ig Δ3 (amino acids 19–140), 30Stalk-Ig Δ7 (amino acids 19–136), and 30Stalk-Ig Δ11 (amino acids 19–132)). The pFUSE-hIgG1-FcQ vector with a 30Stalk insert was used as template to produce glycosylation-deficient mutants of the 30Stalk-Ig protein by site-directed mutagenesis (three single (N42Q, N68Q, and N121Q), three double (N42Q/N68Q, N42Q/121Q, and N68Q/N121Q), and one triple amino acid mutation (N42Q/N68Q/N121Q)). The B7-H6-Ig construct, containing the extracellular domain of B7-H6 (NCBI RefSeq accession number NM_001202439.1) fused C-terminally to an hIgG1-Fc part was provided by C. Watzel (IfADo, Germany). After transfection of 293T cells with the constructs using polyethyleneimine (33), the Ig fusion proteins were purified on Protein A-Sepharose (Invitrogen) from culture supernatant after secretion.

Recombinant NKp30 Receptor Variants—To generate NKp30 receptor constructs, the LeGO-iZ vector was used. The LeGO-iZ vector consists of the LeGO-iG2 backbone (34) where the GFP is exchanged for a Zeocin resistance gene. The full-length gene segment of human NKp30 (NCBI RefSeq accession number NM_147130.2) fused to a C-terminal decahistidine tag (30FL-His) was amplified by PCR from codon usage-optimized cDNA (Genscript) and cloned into the LeGO-iZ vector. The LeGO-iZ vector with the 30FL-His insert was used as a template to produce a stalk domain-truncated (30LBD-His) and a stalk domain GS linker-substituted (30GS-His) NKp30 construct (truncated/substituted residues, 129–135) by overlapping size extension PCR as well as to produce glycosylation-deficient mutants of the 30FL-His insert by site-directed mutagenesis (three single (N42Q, N68Q, and N121Q), three double (N42Q/N68Q, N42Q/121Q, and N68Q/N121Q), and one triple amino acid mutation (N42Q/N68Q/N121Q)).

Generation of Reporter Cell Lines—A5 cells are a CD4-positive T cell hybridoma expressing the 14.3.d T cell receptor β chain (I-E[d], HA110–119, Vα4.2, Vβ8.2) derived from 14.3.d T cell receptor transgenic mice (32). A5 cells were stably transfected with a reporter construct driving GFP expression under the control of three NF-AT binding sites found in the promoter region of the *Il2* gene (A5-GFP) (32, 35). A5-GFP cells were retrovirally transduced with various NKp30 receptor con-
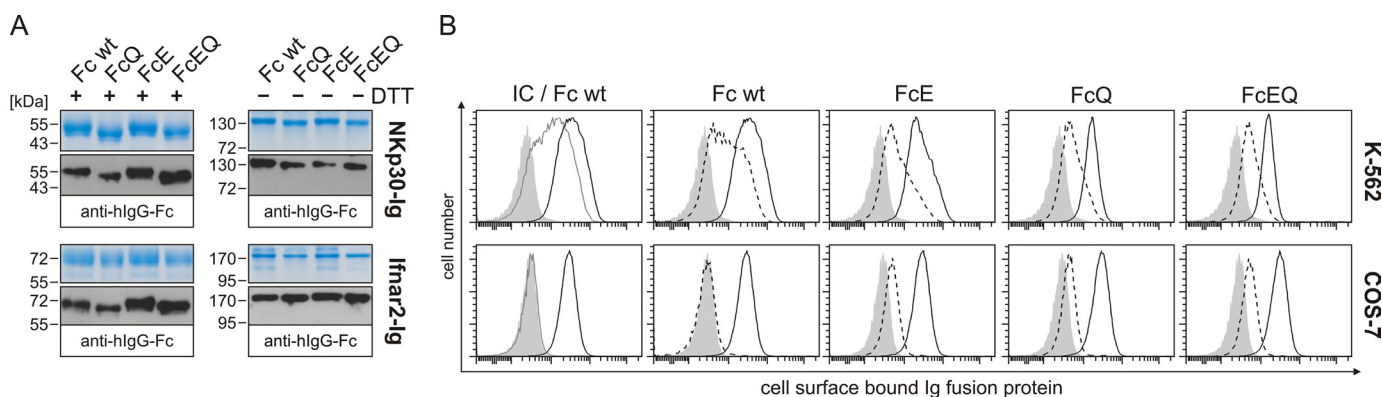
FIGURE 1. **Optimized human NKp30-Ig fusion proteins with reduced binding to FcγR on tumor cells.** *A*, non-reducing (−DTT) and reducing (+DTT) SDS-PAGE (Coomassie-stained) and Western blot (anti-hIgG-Fc) of NKp30 and Ifnar2 ectodomains fused to hIgG1-Fc variants (WT and mutations (N180Q (FcQ), L118E (FcE), and L118E/N180Q (FcEQ)). *B*, flow cytometry of K-562 and COS-7 cells decorated with anti-human IgG-Fc-DyLight 488 (*solid gray*), human isotype control (*IC*; *gray line*), NKp30-Ig variants (*black line*), and Ifnar2-Ig variants (*dashed line*).

structs. Two days after transduction, NKp30 expression was determined by staining with an antibody specific for NKp30 on a flow cytometer. As a control, A5-GFP cells were transfected with empty retrovirus (mock). NKp30-expressing cells were purified using flow cytometry-based cell sorting (MoFlo Astrios, Beckman Coulter). A5-GFP cells and the various NKp30 transductants were maintained in the presence of 0.5 mg/ml hygromycin. The NKp30 receptor associates with CD3ζ expressed by A5-GFP cells. Cognate interaction between the NKp30 receptor and its ligand induces activation of the NF-AT promoter, resulting in GFP expression.

Immunofluorescence Staining—Cells were cultured on glass slides for 48 h, blocked with 3% (w/v) BSA, and incubated with Ig fusion protein (50 μg/ml). After immunostaining (anti-human IgG-Fc-DyLight 488, 7.5 μg/ml) cells were fixed with acetone/methanol (1:1, v/v) and stained with To-Pro-3 ([1 μM]; Invitrogen) prior to microscopy (DM IRBE confocal laser scanning microscope, Leica).

Flow Cytometry—Adherent cells were detached (Accutase, PAA Laboratories), blocked with 5% (w/v) BSA, and incubated with Ig fusion protein (50 μg/ml). After immunostaining (anti-human IgG-Fc-DyLight 488, 7.5 μg/ml), cells were fixed with 1% (v/v) formaldehyde, and a minimum of 50,000 cells were analyzed with a FACSCanto II instrument and BD Diva 6.0 software (BD Biosciences). Statistical significance was determined by the Mann-Whitney test using Prism 5 software (GraphPad): not significant, >0.05; *, $p = 0.01–0.05$; **, $p = 0.001–0.01$; and ***, $p < 0.001$.

ELISAs—96-well ELISA plates (Greiner) were coated with recombinant BAG-6 protein (1 μg/well), blocked with 5% (w/v) BSA, and incubated with graded amounts of Ig fusion proteins (0–10 μg/well). The amount of bound Ig fusion proteins was quantified after immunodetection (anti-human IgG-Fc) and visualization with *3,3′,5,5′-tetramethylbenzidine* substrate in a microtiter plate reader (λ = 450 nm). K_D and B_{max} values were determined by fitting the curves to a 1:1 Langmuir binding model using Prism 5 software (GraphPad).

Surface Plasmon Resonance (SPR)—The interaction of B7-H6-Ig and NKp30-Ig variants was assessed by SPR using the ProteOn XPR36 protein interaction array system (Bio-Rad). Typically, 6,000–11,000 resonance units of NKp30-Ig variants

were immobilized on a GLC sensor chip by random amine coupling. Different analyte concentrations of B7-H6-Ig were injected sequentially over the microfluidic cells immobilized with NKp30-Ig variants or buffer as a blank. The data were analyzed using ProteOn Manager 3.1.0 software (Bio-Rad). K_D values were determined from bivalent analyte analysis after correction for the interspot data.

Signaling Reporter Assays—A5-GFP effector cells were mixed with 50,000 Ba/F3-B7-H6 target cells at effector:target ratios of 2:1, 1:1, and 0.5:1. After 16 h of co-incubation at 37 °C, cells were stained with a CD4-specific antibody, and GFP expression of CD4^{+} A5 cells was determined on a flow cytometer. As a positive control, A5 cells were incubated for 16 h in the presence of 50 ng/ml PMA and 750 ng/ml ionomycin.

RESULTS

Optimized Human NKp30-Ig Fusion Proteins with Reduced Binding to Fc Receptors—Bivalent fusion proteins of the ectodomain of NK cell receptors with the IgG1-Fc part of human immunoglobulins (hIgG1-Fc) are a valuable tool to study receptor-ligand interactions *in vitro* (16, 24, 36). However, as a major drawback, these constructs display an inherent binding activity to the Fcγ receptor (FcγR) on target cells via their Ig domains and thus limited potential to investigate the actual receptor-ligand interaction. To overcome this limitation, we mutated leucine 118 to glutamate (L118E; FcE) and removed a glycosylation acceptor site (mutation of asparagine 180 to glutamine (N180Q; FcQ)) within hIgG1-Fc, both of which are essential for FcγR binding (37–40). Fusion proteins of the ectodomain of NKp30 and the novel hIgG1-Fc variants were generated and affinity-purified to homogeneity on Protein A (2 mg of pure protein from 10^8 cells) after secretion into the culture medium of 293T cells (Fig. 1*A*). For reference, the ectodomain of the human interferon receptor subunit Ifnar2 was fused to the hIgG1-Fc variants as well and produced accordingly. All of the Ig fusion proteins form disulfide-linked homodimers as shown by reducing and non-reducing SDS-PAGE and corresponding Western blot analyses. The fusion proteins with an FcQ mutation display a lower apparent molecular mass than their wild-type (WT) counterparts, demonstrating deficiency in glycosylation due to removal of the glycosylation targeting

site. The ligand binding properties of the various Ig fusion proteins were assayed by flow cytometry on K-562 cells, which express a cellular ligand of NKp30 (19, 24, 41) and high levels of FcγR (42, 43) (Fig. 1B). As detailed above, human NKp30 fused to a WT hIgG1-Fc (NKp30-Ig Fc WT) bound only slightly more strongly to the cell surface of K-562 cells when compared with the analogous Ifnar2 reference construct (Ifnar2-Ig Fc WT) or the IgG1 isotype control. By contrast, fusion proteins with the mutated hIgG1-Fc variants (FcE, FcQ, and FcEQ) displayed reduced background binding, thus enabling the exclusive investigation of NKp30 binding to its cellular ligands. Interestingly, the double mutant (FcEQ) showed about the same reduction in background binding as the single mutants (FcQ and FcE), suggesting sufficiency of the individual mutations. For reference, the optimized Ig fusion constructs were tested for binding to COS-7 cells, which express ligands of NKp30 (41) but no human FcγR. The determined binding patterns resemble those observed for K-562 cells, demonstrating quantitative background reduction (Fig. 1B). Based on these results, the optimized NKp30-Ig variants are validated tools for the investigation of NKp30-dependent ligand binding, and the optimized hIgG1-Fc scaffolds were used to generate further NKp30-Ig fusion proteins throughout the current study.

The Stalk Domain of NKp30 Impacts Ligand Binding—Part of the ectodomain of NKp30 (amino acids 19–128) adopts an Ig-like fold (29, 30), providing a binding pocket for B7-H6 at its membrane-distal face (30). Although the stalk domain connecting the closed fold of the LBD of NKp30 with the TMD region was not resolved in the crystal structure, its N-terminal end was defined. The border between the stalk domain and the TMD was predicted using TMpred (44), thus defining a stretch of 15 amino acids that comprise the stalk domain (amino acids 129–143). To investigate whether the stalk domain impacts ligand binding of NKp30, we generated Ig fusion proteins containing either the LBD alone (30LBD-Ig) or the complete ectodomain of NKp30 including the stalk domain (30Stalk-Ig). These proteins were purified to homogeneity on Protein A after secretion into the culture medium of transiently transfected 293T cells (Fig. 2, A and B). The NKp30-Ig as well as the Ifnar2-Ig fusion protein assembles into bivalent disulfide-bridged homodimers as demonstrated by reducing and non-reducing SDS-PAGE and corresponding Western blot analyses with human IgG-Fc- and human NKp30-specific antibodies (Fig. 2C). As expected, the apparent molecular mass of the 30LBD-Ig construct is slightly lower than that of the 30Stalk-Ig construct due to the missing stalk region (Fig. 2C). The ligand binding properties of the 30LBD-Ig and 30Stalk-Ig constructs were evaluated in cell decoration experiments by immunofluorescence microscopy and flow cytometry (Fig. 2, D and E). Strikingly, the 30Stalk-Ig construct bound more strongly to ligands on target cells than the 30LBD-Ig construct, demonstrating a significant contribution of the stalk domain of NKp30 to ligand binding. This effect was confirmed on a panel of several cell lines of different tissue and species origins (Fig. 2F, supplemental Table S1, and supplemental Fig. S1). Importantly, none of the constructs bound to the surface of cells, which does not express NKp30 ligands, demonstrating ligand-dependent binding (Fig. 2G and supplemental Fig. S1). Notably, expression

of the NKp30 ligand B7-H6 in the NKp30 ligand-negative cell line Ba/F3 (Ba/F3-B7-H6) led to NKp30-specific cell decoration, confirming a significant contribution of the stalk domain of NKp30 to ligand binding (Fig. 2G). Because the ligand(s) recognized in cell decoration experiments on tumor cells are ill-defined, we established an ELISA-based assay to study the molecular details of NKp30 binding to its ligand BAG-6 found on tumor cells and DCs (17, 18). Additionally, the interaction of NKp30 and its ligand B7-H6 was analyzed in molecular detail using SPR. All of the NKp30-Ig fusion proteins bound specifically to recombinant BAG-6 and B7-H6 proteins, demonstrating correct assembly and folding (Fig. 2H and Fig. 3, A and B). In accordance with results from the cell decoration experiments (see above), the equilibrium binding constant (K_D) of the 30Stalk-Ig construct (BAG-6, 48 ± 5 nM; B7-H6, 76 ± 20 nM) was significantly lower than that of the 30LBD-Ig construct (BAG-6, 126 ± 14 nM; B7-H6, 149 ± 19 nM), confirming the importance of the stalk domain for ligand binding of NKp30.

The Integrity of the Stalk Domain Is Important for Ligand Binding of NKp30—To further characterize the contribution of the stalk domain to ligand binding by NKp30, we generated an NKp30-Ig fusion construct containing a length-matched GS linker instead of the stalk domain (30GS-Ig). Ligand binding of the 30GS-Ig protein was investigated by flow cytometry on several cell lines of different tissue and species origins. Notably, the GS linker could not substitute for the intrinsic stalk domain of NKp30 as binding of the 30GS-Ig construct was comparable with the NKp30 construct without the stalk domain (Fig. 4A and supplemental Fig. S2). Surprisingly, the 30GS-Ig construct showed an intermediate phenotype for the Ba/F3-B7-H6 cells when compared with the 30LBD-Ig and 30Stalk-Ig constructs (Fig. 4B and supplemental Fig. S2). To validate this observation, we determined the K_D of the 30GS-Ig construct for binding to BAG-6 by ELISA (Fig. 4C) and to B7-H6 by SPR (Fig. 3C). The determined K_D of the 30GS-Ig construct (BAG-6, 86 ± 7 nM; B7-H6, 114 ± 9 nM) was found to be in between those for the 30Stalk-Ig (BAG-6, 48 ± 5 nM; B7-H6, 76 ± 20 nM) and the 30LBD-Ig construct (BAG-6, 126 ± 14 nM; B7-H6, 149 ± 19 nM), confirming the results from the cell decoration experiments with Ba/F3-B7-H6 cells (see above). Based on these data, we conclude that the amino acid composition of the stalk domain is important for ligand recognition and that the stalk domain contributes directly to ligand binding rather than acting solely as a flexible spacer for the LBD.

To determine the minimal functional requirements of the stalk domain, we generated 30Stalk-Ig proteins C-terminally truncated by 3 (30Stalk-Ig Δ3), 7 (30Stalk-Ig Δ7), or 11 (30Stalk-Ig Δ11) amino acids. Ligand binding of these constructs was analyzed by flow cytometry on several cell lines of different tissue and species origins. Surprisingly, all of the truncated NKp30-Ig constructs lost the superior ligand binding properties of the 30Stalk-Ig construct as demonstrated by a binding phenotype comparable with the NKp30 construct without the stalk domain (Fig. 5A and supplemental Fig. S3A). Notably, this effect was less pronounced for cell decoration experiments with Ba/F3-B7-H6 (Fig. 5B and supplemental Fig. S3A), correlating with the K_D value determination of the 30Stalk-Ig truncation variants for binding to B7-H6 (SPR)
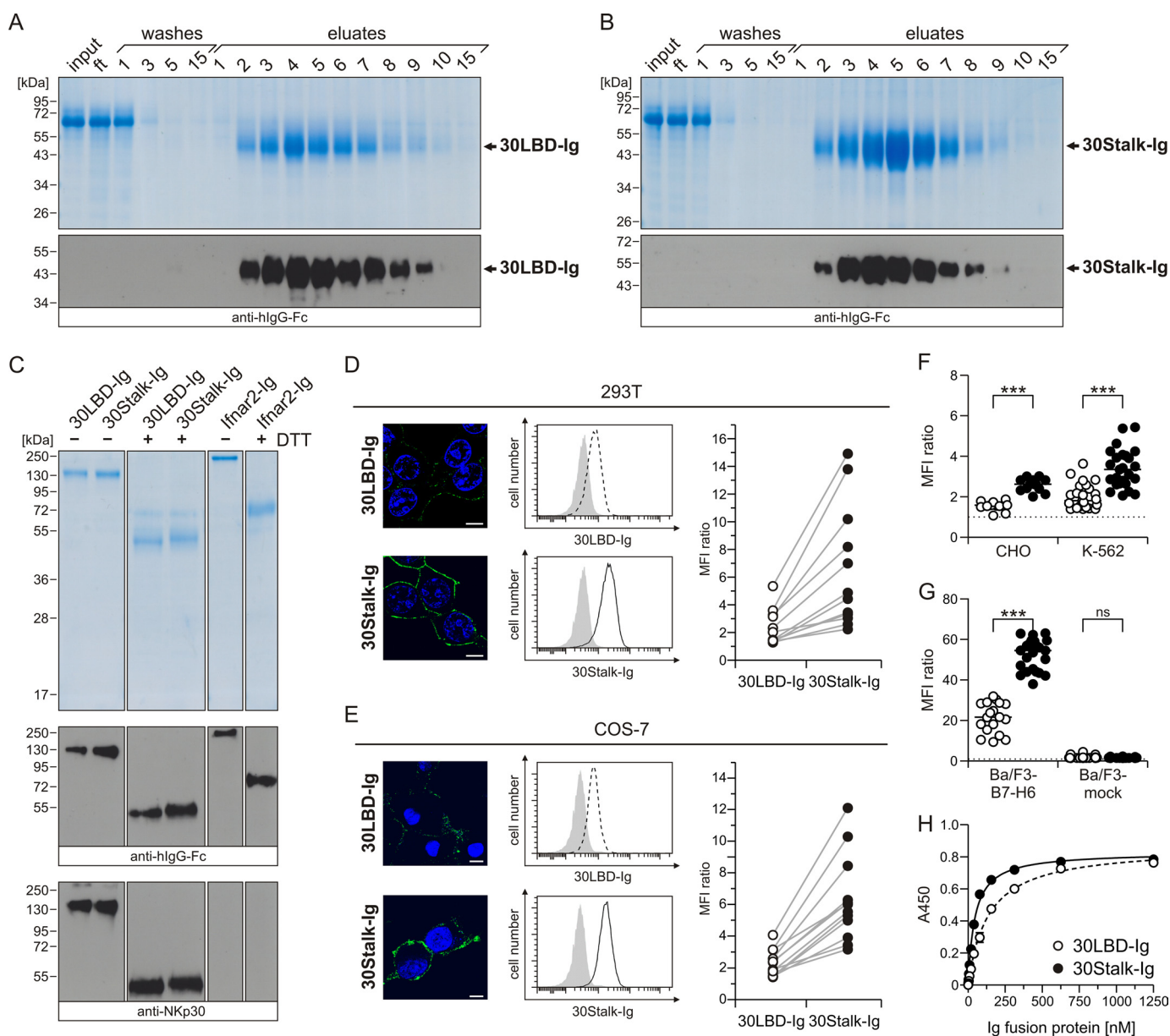
FIGURE 2. **Importance of the stalk domain of NKp30 for ligand binding.** *A* and *B*, shown are reducing SDS-PAGE (Coomassie-stained) and Western blot (anti-hIgG-Fc) of aliquots (input, flow-through (*ft*), washes, and eluates) from purification of 30LBD-Ig (without stalk; *A*) and 30Stalk-Ig (entire ectodomain; *B*) proteins. *C*, non-reducing (−DTT) and reducing (+DTT) SDS-PAGE (Coomassie-stained) and Western blot (anti-hIgG-Fc and anti-NKp30) of purified 30LBD-Ig, 30Stalk-Ig, and Ifnar2-Ig proteins. *D* and *E*, 293T and COS-7 cells were decorated with 30LBD-Ig and 30Stalk-Ig proteins and analyzed by immunofluorescence microscopy (Ig fusion protein, *green*; To-Pro-3, *blue*) and flow cytometry (30LBD-Ig, *dashed line*; 30Stalk-Ig, *black line*; Ifnar2-Ig, *solid gray*). A representative measurement is shown as a histogram (*middle*), and the median fluorescence intensities (*MFI*; divided by the median fluorescence intensity of Ifnar2-Ig background staining) of 12 independent measurements are plotted (*right*). *F* and *G*, same flow cytometry experiment as in *D* and *E* with CHO and K-562 cells and Ba/F3 cells either transduced with the NKp30 ligand B7-H6 (Ba/F3-B7-H6) or with GFP as control (Ba/F3-mock). *H*, binding of graded amounts of 30LBD-Ig (*open circles*) and 30Stalk-Ig (*black circles*) proteins to recombinant BAG-6 by ELISA. Data were corrected for Ifnar2-Ig background binding and fitted to a 1:1 Langmuir binding model to determine K_D and B_{max} values. A representative of three independent experiments is shown. *ns*, not significant, >0.05; ***, $p < 0.001$.

(30Stalk-Ig Δ3, 132 ± 36 nM; 30Stalk-Ig Δ7, 133 ± 36 nM; 30Stalk-Ig Δ11, 137 ± 27 nM) (Figs. 5*C* and 3, *D–F*). Importantly, there is no nonspecific binding of B7-H6 during surface plasmon resonance measurements (Fig. 2, *N* and *O*). Moreover, the K_D values of the 30Stalk-Ig truncation variants for binding to BAG-6 (ELISA) were similar to those observed for the 30GS-Ig construct with a GS linker-substituted stalk domain (30Stalk-Ig Δ3, 79 ± 7 nM; 30Stalk-Ig Δ7, 62 ± 12 nM; 30Stalk-Ig Δ11, 93 ± 20 nM) (Fig. 5*C* and supplemental Fig. S3B). All of the receptor fusion proteins were expressed in a human cell line

and were purified from culture supernatant after secretion. Therefore, they have passed all of the quality control check points of the cell including endoplasmic reticulum and Golgi. Moreover, the constructs show different K_D values (different affinities) for their corresponding ligands but preserved B_{max} values. The B_{max} value is indicative for the total amount of binding sites within the protein solution. Because all of the binding experiments were performed with the same amount of protein, the identical B_{max} values are indicative for a correct ligand binding-receptive conformation of the receptor variants.
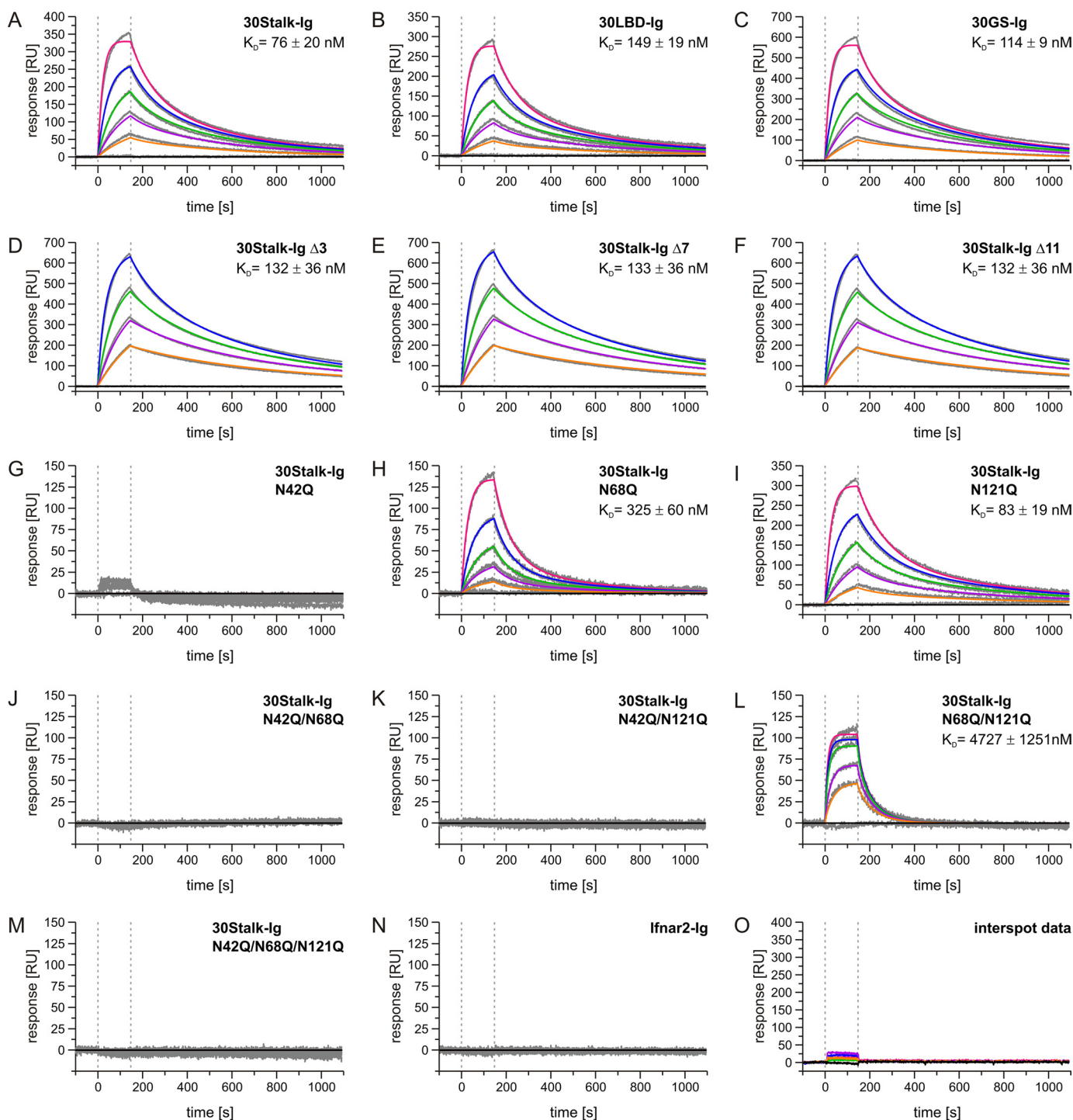
FIGURE 3. **Equilibrium binding of NKp30 variants and B7-H6.** Shown are SPR sensorgrams for the interaction of B7-H6-Ig fusion protein with immobilized NKp30-Ig fusion variants and Ifnar2-Ig as control. *A*, 30Stalk-Ig WT (8850 RU)/B7-H6-Ig (250, 100, 50, 25, 10, and 0 nM). *B*, 30LBD-Ig (9700 RU)/B7-H6-Ig (250, 100, 50, 25, 10, and 0 nM). *C*, 30GS-Ig (10,000 RU)/B7-H6-Ig (250, 100, 50, 25, 10, and 0 nM). *D*, 30Stalk-Ig Δ3 (8300 RU)/B7-H6-Ig (250, 100, 50, 25, and 0 nM). *E*, 30Stalk-Ig Δ7 (7800 RU)/B7-H6-Ig (250, 100, 50, 25, and 0 nM). *F*, 30Stalk-Ig Δ11 (6800 RU)/B7-H6-Ig (250, 100, 50, 25, and 0 nM). *G*, 30Stalk-Ig N42Q (7676 RU)/B7-H6-Ig (1500, 1250, 1000, 500, 250, and 0 nM). *H*, 30Stalk-Ig N68Q (10,100 RU)/B7-H6-Ig (250, 100, 50, 25, 10, and 0 nM). *I*, 30Stalk-Ig N121Q (10,100 RU)/B7-H6-Ig (250, 100, 50, 25, 10, and 0 nM). *J*, 30Stalk-Ig N42Q/N68Q (7800 RU)/B7-H6-Ig (250, 100, 50, 25, 10, and 0 nM). *K*, 30Stalk-Ig N42Q/N121Q (9800 RU)/B7-H6-Ig (1500, 1250, 1000, 500, 250, and 0 nM). *L*, 30Stalk-Ig N68Q/N121Q (10,800 RU)/B7-H6-Ig (1500, 1250, 1000, 500, 250, and 0 nM). *M*, 30Stalk-Ig N42Q/N68Q/N121Q (9400 RU)/B7-H6-Ig (1500, 1250, 1000, 500, 250, and 0 nM). *N*, Ifnar2-Ig (4800 RU)/B7-H6-Ig (1500, 1250, 1000, 500, 250, and 0 nM). The *gray lines* represent the data corrected for the interspot data and were fitted to a bivalent binding model (*colored lines*) to determine K_D values. A representative of at least three independent experiments is shown. The RU values behind the construct names indicate the amount of immobilized protein. *O*, representative interspot data of 30Stalk-Ig WT/B7-H6-Ig demonstrating no nonspecific binding to the surface.

In summary, these data demonstrate that optimal ligand binding of NKp30 depends on the integrity of the stalk domain with respect to sequence composition and length. Most importantly, impaired ligand binding of the 30Stalk-Ig mutants is a consequence of a reduced binding affinity rather than differences in the proportion of binding-receptive receptors within the pop-
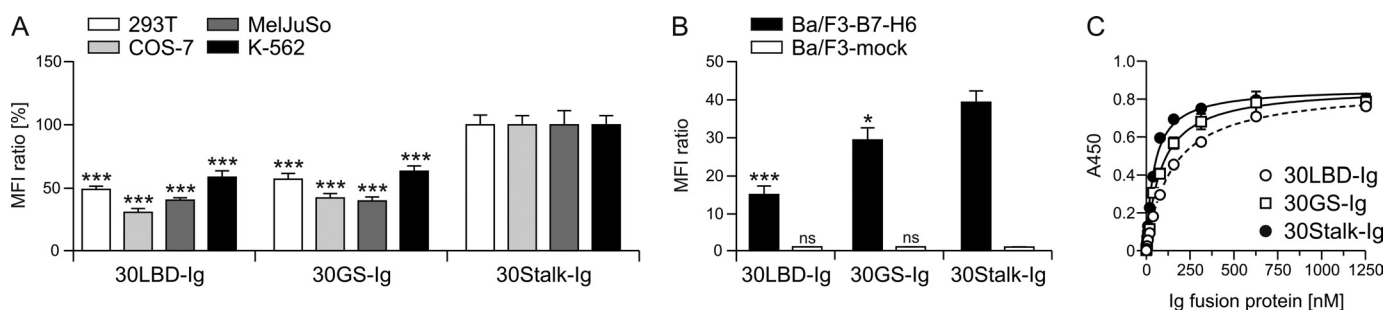
FIGURE 4. **Substitution of the stalk domain reduces the ligand binding affinity of NKp30.** *A* and *B*, 293T, COS-7, K-562, and MelJuSo cells (*A*) as well as Ba/F3 cells either transduced with the NKp30 ligand B7-H6 (Ba/F3-B7-H6) or with GFP as a control (Ba/F3-mock) (*B*) were decorated with 30LBD-Ig, 30GS-Ig (stalk substituted by GS linker), and 30Stalk-Ig proteins and analyzed by flow cytometry. Median fluorescence intensity (*MFI*) ratios were determined as described in Fig. 2, *D* and *E* (*A* and *B*), and normalized to 30Stalk-Ig (*A*). The median fluorescence intensity ratios of seven or more independent experiments are plotted. *C*, BAG-6 ELISA with 30LBD-Ig (*open circles*), 30GS-Ig (*open squares*), and 30Stalk-Ig (*black circles*) proteins (compare Fig. 2*H*). A representative of three independent experiments is shown. *ns*, not significant, >0.05; *, $p = 0.01–0.05$; ***, $p < 0.001$. *Error bars* represent S.E.
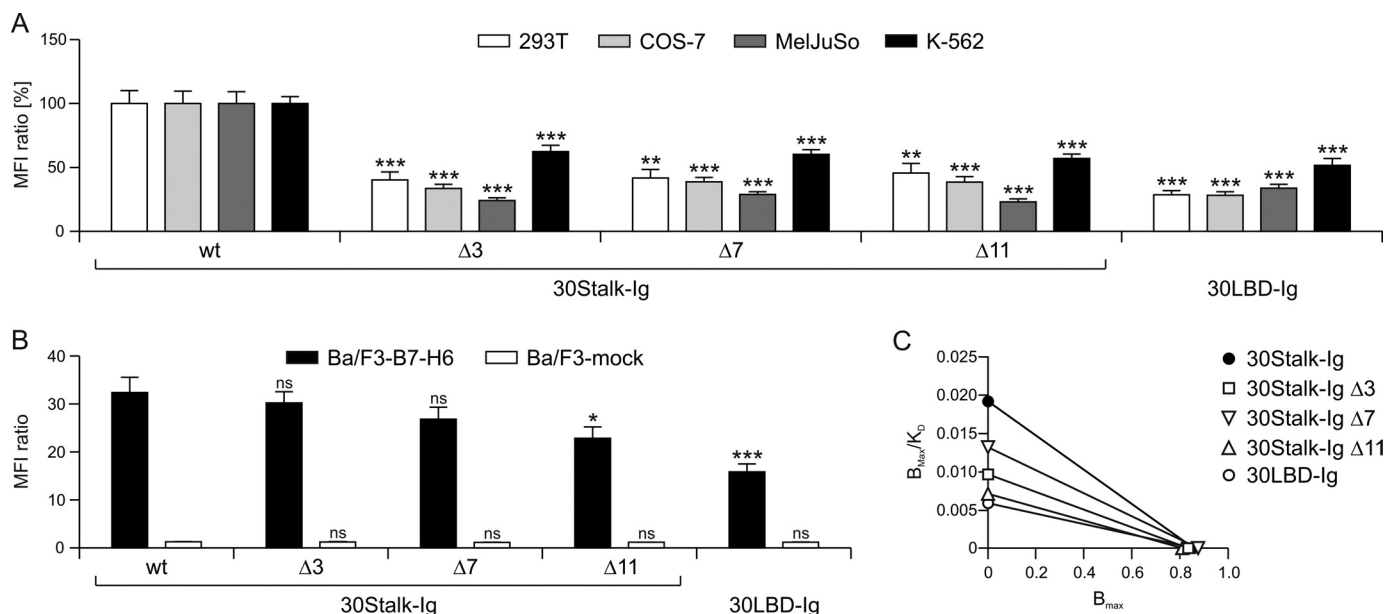

FIGURE 5. **The stalk domain of NKp30 is sensitive to C-terminal truncation.** *A* and *B*, 293T, COS-7, K-562, and MelJuSo cells (*A*) as well as Ba/F3 cells either transduced with the NKp30 ligand B7-H6 (Ba/F3-B7-H6) or with GFP as a control (Ba/F3-mock) (*B*) were decorated with 30LBD-Ig; 30Stalk-Ig variants C-terminally truncated by 3 (30Stalk-Ig Δ3), 7 (30Stalk-Ig Δ7), or 11 (30Stalk-Ig Δ11) amino acids; or 30Stalk-Ig and analyzed by flow cytometry (compare Fig. 4). *C*, BAG-6 ELISA with 30LBD-Ig, 30Stalk-Ig Δ3, 30Stalk-Ig Δ7, 30Stalk-Ig Δ11, or 30Stalk-Ig protein. Data were fitted according to Fig. 2*H* and are shown as a Scatchard plot to visualize the different K_D but identical B_{max} values of the individual constructs. A representative of three independent experiments is shown. *ns*, not significant, >0.05; *, $p = 0.01–0.05$; **, $p = 0.001–0.01$; ***, $p < 0.001$. *Error bars* represent S.E. *MFI*, median fluorescence intensity.

ulation (*e.g.* because of folding deficiencies) as demonstrated by preservation of the B_{max} values.

N-Linked Glycosylation of NKp30 Modulates Ligand Binding—Because the predicted molecular mass of the ectodomain of NKp30 (roughly 14 kDa) differs significantly from its appearance in reducing SDS-PAGE (roughly 25 kDa), we hypothesized that NKp30 is glycosylated. To address this question, the purified 30LBD-Ig and 30Stalk-Ig proteins were subjected to deglycosylation with peptide-*N*-glycosidase F (removal of *N*-linked glycans) or a mixture of glycosidases (removal of *N*- and *O*-linked glycans) prior to reducing SDS-PAGE and Western blot analyses. Upon peptide-*N*-glycosidase F treatment, both proteins shifted to their molecular mass predicted from the primary sequence (roughly 39 kDa including the Ig domain of 25 kDa), demonstrating that the ectodomain of NKp30 is *N*-linked glycosylated (Fig. 6*A*). Because treatment of the pro-

teins with the glycosidase mixture produced no further size shift, *O*-linked glycosylation of NKp30 was formally excluded.

Three potential acceptor sites for *N*-linked glycosylation (N*X*(S/T) consensus motif) were predicted from the primary sequence of NKp30. To investigate which of these sites is glycosylated *in vivo*, NKp30-Ig proteins with a defined set of acceptor site(s) (three single mutations (N42Q, N68Q, and N121Q), three double mutations (N42Q/N68Q, N42Q/N121Q, and N68Q/N121Q), and one triple mutation (N42Q/N68Q/N121Q)) were generated as described above. Assembly of bivalent disulfide-bridged homodimers was demonstrated for all constructs by reducing and non-reducing SDS-PAGE (Fig. 6*B* and supplemental Fig. S4). Interestingly, successive deletion of potential acceptor sites for *N*-linked glycosylation went along with a stepwise reduction of the apparent molecular mass of the 30Stalk-Ig mutants (Fig. 6, *B* and *C*). Moreover,
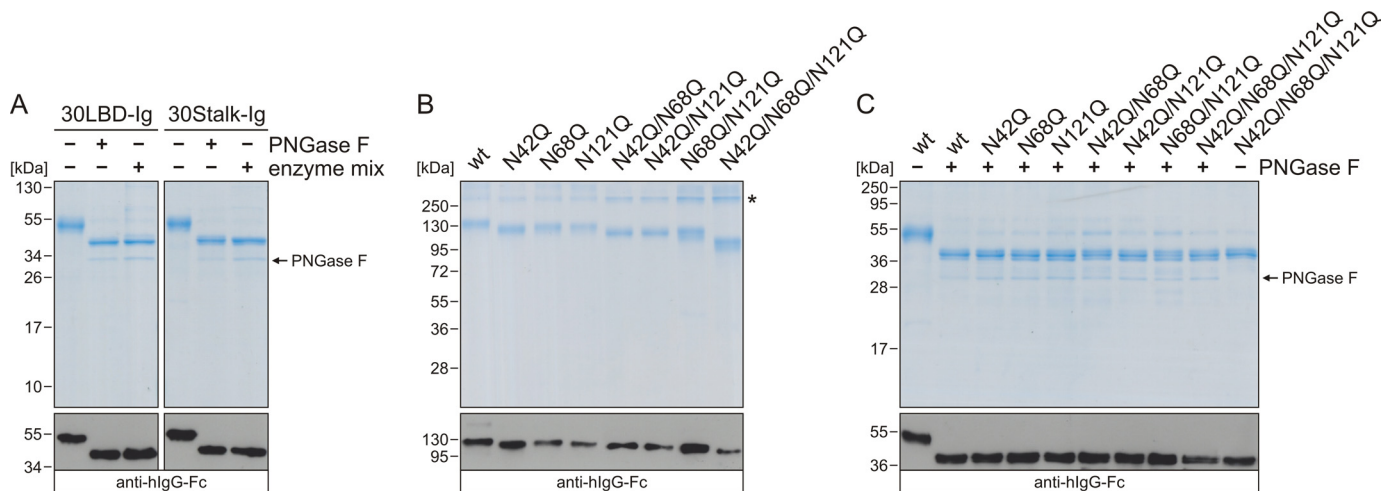
FIGURE 6. **The ectodomain of NKp30 is *N*-linked glycosylated at three sites.** *A*, reducing SDS-PAGE (Coomassie-stained) and Western blot (anti-hIgG-Fc) analysis of deglycosylated 30LBD-Ig and 30Stalk-Ig. *B*, non-reducing SDS-PAGE (Coomassie-stained) and Western blot (anti-hIgG-Fc) analysis of purified 30Stalk-Ig variants (WT and three single (N42Q, N68Q, and N121Q), three double (N42Q/N68Q, N42Q/121Q, and N68Q/N121Q), and one triple amino acid mutation (N42Q/N68Q/N121Q)). An *asterisk* indicates traces of serum albumin in the sample. *C*, reducing SDS-PAGE (Coomassie-stained) and Western blot (anti-hIgG-Fc) analysis of deglycosylated 30Stalk-Ig variants. Peptide-*N*-glycosidase F (*PNGaseF*) (removal of *N*-linked glycans); enzyme mix (removal of *N*- and *O*-linked glycans; protein deglycosylation mix, P6039S, New England Biolabs).

peptide-*N*-glycosidase F treatment shifted the apparent molecular mass of all 30Stalk-Ig mutants to that of the glycosylation-deficient triple mutant (Fig. 6*C*).

To investigate the ligand binding properties of the differentially glycosylated 30Stalk-Ig mutants, they were analyzed by immunofluorescence microscopy and flow cytometry in cell decoration experiments with NKp30 ligand-positive cell lines of different tissue and species origins. Specific staining was found for all mutants with varying intensity (Fig. 7 and supplemental Fig. S5). No altered binding phenotype could be detected for K-562 cells. Interestingly, all diglycosylated and some monoglycosylated (N68Q and N121Q) mutants showed improved ligand binding to 293T, COS-7, and MelJuSo cells when compared with the 30Stalk-Ig WT construct. By contrast, the triple mutant of the 30Stalk-Ig construct devoid of *N*-linked glycans displayed the same binding phenotype when compared with 30Stalk-Ig WT protein (Fig. 7*B* and supplemental Fig. S5). These results correlate with the different affinities (K_D) of the 30Stalk-Ig mutants for binding to BAG-6 as measured by ELISA (Table 1 and supplemental Fig. S6). Notably, the B_{max} values of the constructs for binding to BAG-6 were preserved. Surprisingly, on Ba/F3-B7-H6 cells, all monoglycosylated mutants except glycosylation mutant N121Q and diglycosylated mutants as well as the triple mutant showed a reduced ligand binding phenotype when compared with the 30Stalk-Ig WT construct (Fig. 7*C* and supplemental Fig. S5). These results correlate with the different affinities (K_D) of the 30Stalk-Ig mutants for binding to B7-H6 as measured by SPR (Table 2 and Fig. 3, *A* and *G–M*). Notably, binding of NKp30 to B7-H6 was abrogated by destroying glycosylation site Asn-42.

The Stalk Domain and the Glycosylation Status of NKp30 Impact Intracellular Signaling—Because NKp30 possesses no signaling motif within its short cytoplasmic tail, NKp30 associates with the signaling adaptor protein CD3ζ via an opposing charge contact in the TMD. To analyze whether the observed binding phenotype of the various NKp30-Ig fusion constructs

directly correlates with the signaling capacity of corresponding full-length receptors in a cellular context, we expressed the various NKp30 receptor variants in a CD3ζ reporter cell line. In this cell line, CD3ζ signaling can be monitored by induced GFP expression.

To determine the influence of the stalk domain of NKp30 on CD3ζ signaling, we generated variants of the NKp30 receptor (30FL-His) without the stalk domain (30LBD-His) or with a length-matched GS linker instead of the stalk domain (30GS-His). The relative NKp30 surface expression was quantified by flow cytometry, demonstrating similar expression levels of the constructs and most importantly successful targeting to the plasma membrane (Fig. 8*A*). To investigate the signaling capacity of the NKp30 receptor variants, the reporter cell lines were incubated with Ba/F3 cells stably transduced with B7-H6. The 30FL-His receptor showed CD3ζ signaling in accordance with the different effector:target ratios used, whereas the NKp30 receptor without the stalk domain (30LBD-His) was impaired in signaling (Fig. 8, *B* and *C*). Furthermore, the 30GS-His receptor failed to stimulate signaling via CD3ζ, confirming the results of the NKp30-Ig fusion binding studies, but with an even more drastic phenotype (Fig. 8, *A* and *B*). The observed differences are unlikely to be reflective of the reduced surface levels of the stalk mutants because reporter cells expressing wild-type NKp30 at even lower levels than the stalk mutants still showed appreciable signaling (data not shown). For reference, stimulation with PMA/ionomycin led to robust CD3ζ signaling for all NKp30 receptor cell lines (Fig. 8*B*).

To investigate the signaling properties of differentially glycosylated 30FL-His receptors, glycosylation-deficient NKp30 receptor variants with a defined set of acceptor site(s) for *N*-linked glycosylation (three single mutations (N42Q, N68Q, and N121Q), three double mutations (N42Q/N68Q, N42Q/N121Q, and N68Q/N121Q), and one triple mutation (N42Q/N68Q/N121Q)) were generated as described above. Surface expression of the glycosylation-deficient NKp30 receptor
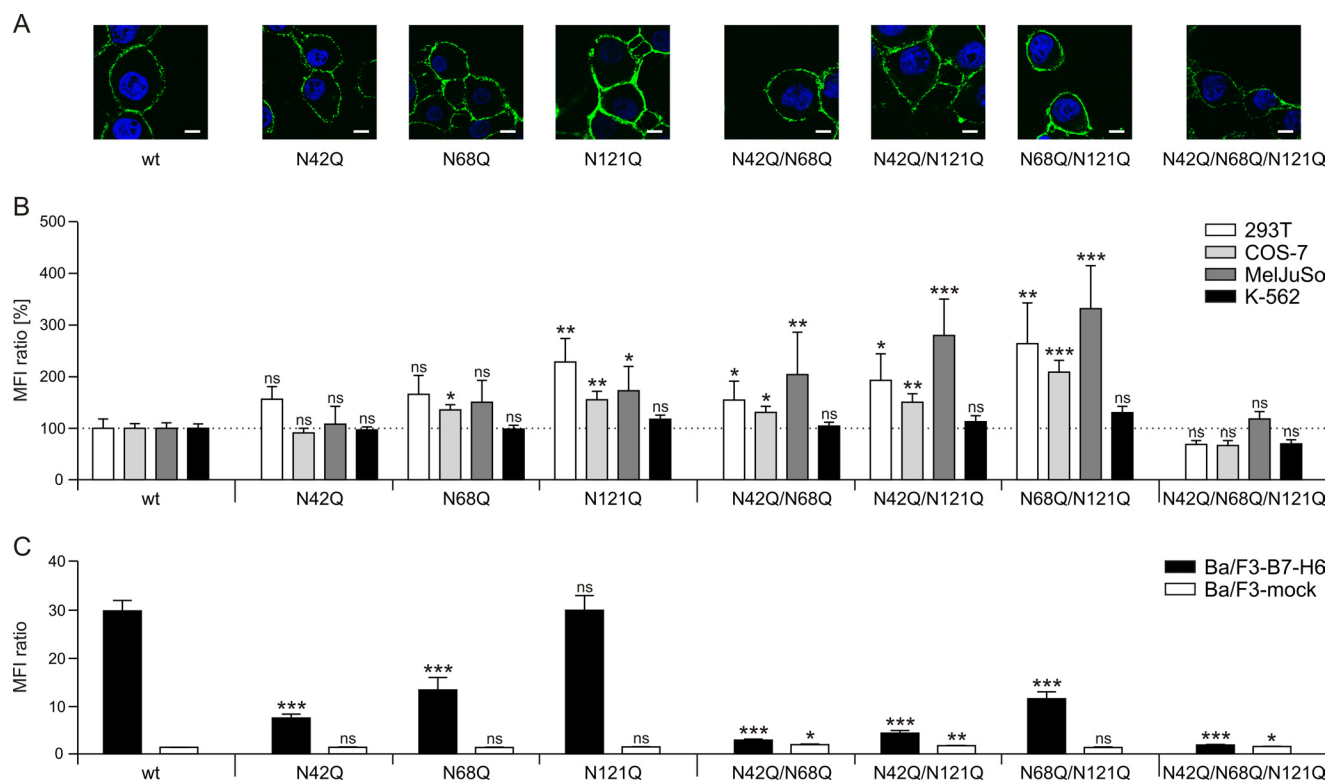
FIGURE 7. **The glycosylation status of NKp30 influences ligand binding.** *A*, COS-7 cells were decorated with 30Stalk-Ig variants (WT and three single (N42Q, N68Q, and N121Q), three double (N42Q/N68Q, N42Q/121Q, and N68Q/N121Q), and one triple amino acid mutation (N42Q/N68Q/N121Q)) and analyzed by immunofluorescence microscopy (Ig fusion protein, *green*; To-Pro-3, *blue*). *B* and *C*, various cell lines (*B*) as well as Ba/F3 cells either transduced with the NKp30 ligand B7-H6 (Ba/F3-B7-H6) or with GFP as a control (Ba/F3-mock) (*C*) were decorated with the 30Stalk-Ig variants and analyzed by flow cytometry (compare Fig. 4). *ns*, not significant, >0.05; *, $p = 0.01$–0.05; **, $p = 0.001$–0.01; ***, $p < 0.001$. *Error bars* represent S.E. *MFI*, median fluorescence intensity.

TABLE 1

Equilibrium binding constants (K_D) of 30Stalk-Ig variants to BAG-6 as determined by ELISA

For experimental details refer to supplemental Fig. S6.

30Stalk-Ig variant	K_D
	nM
WT	48 ± 5
N42Q	26 ± 4
N68Q	14 ± 2
N121Q	24 ± 1
N42Q/N68Q	21 ± 4
N42Q/N121Q	22 ± 8
N68Q/N121Q	18 ± 5
N42Q/N68Q/N121Q	54 ± 17

TABLE 2

Equilibrium binding constants (K_D) of 30Stalk-Ig variants to B7-H6 as determined by SPR

For experimental details refer to Fig. 3.

30Stalk-Ig variant	K_D
WT	76 ± 20 nM
N42Q	>10 μM
N68Q	325 ± 60 nM
N121Q	83 ± 19 nM
N42Q/N68Q	>10 μM
N42Q/N121Q	>10 μM
N68Q/N121Q	3323 ± 326 nM
N42Q/N68Q/N121Q	>10 μM

mutants was analyzed by flow cytometry, confirming similar expression levels for all constructs and successful targeting to the plasma membrane (Fig. 9*A*). Notably, the triple mutant (N42Q/N68Q/N121Q) was not detectable. Incubation of reporter cell lines expressing glycosylation variants of NKp30

with Ba/F3-B7-H6 cells revealed that all diglycosylated mutants as well as the monoglycosylated mutants N42Q and N68Q show a reduced signaling capacity when compared with 30FL-His (Fig. 9, *B* and *C*). For reference, stimulation with PMA/ionomycin led to robust CD3ζ signaling for all NKp30 receptor cell lines (Fig. 9*B*). In accordance with binding studies of NKp30-Ig fusion proteins to Ba/F3-B7-H6 cells, glycosylation at residues Asn-42 and Asn-68 is critical for NKp30 function, whereas glycosylation at Asn-121 has little influence on ligand binding and signaling of NKp30 (Fig. 9, *C* and *B*). In conclusion, these data demonstrate that the ectodomain of NKp30 is differentially *N*-linked glycosylated at all three consensus motifs within the LBD in the plasma membrane of living cells. The glycosylation status of NKp30 influences its ligand binding affinity and signaling capacity. Therefore, the glycosylation status of NKp30 may be a way to tune ligand recognition and NKp30-dependent NK cell cytotoxicity. In this context, Asn-42 and Asn-68 play a major role.

DISCUSSION

NK cell cytotoxicity against tumor cells and the cross-talk of NK cells with DCs depend largely on NKp30. However, little is known about the molecular determinants of ligand recognition. Previous studies were performed with Ig fusion proteins of a partial ectodomain of NKp30 (16, 24, 41). These constructs display an inherent binding activity to the FcγR on target cells via their Ig domains and thus have limited potential to investigate the actual receptor-ligand interaction. To overcome this
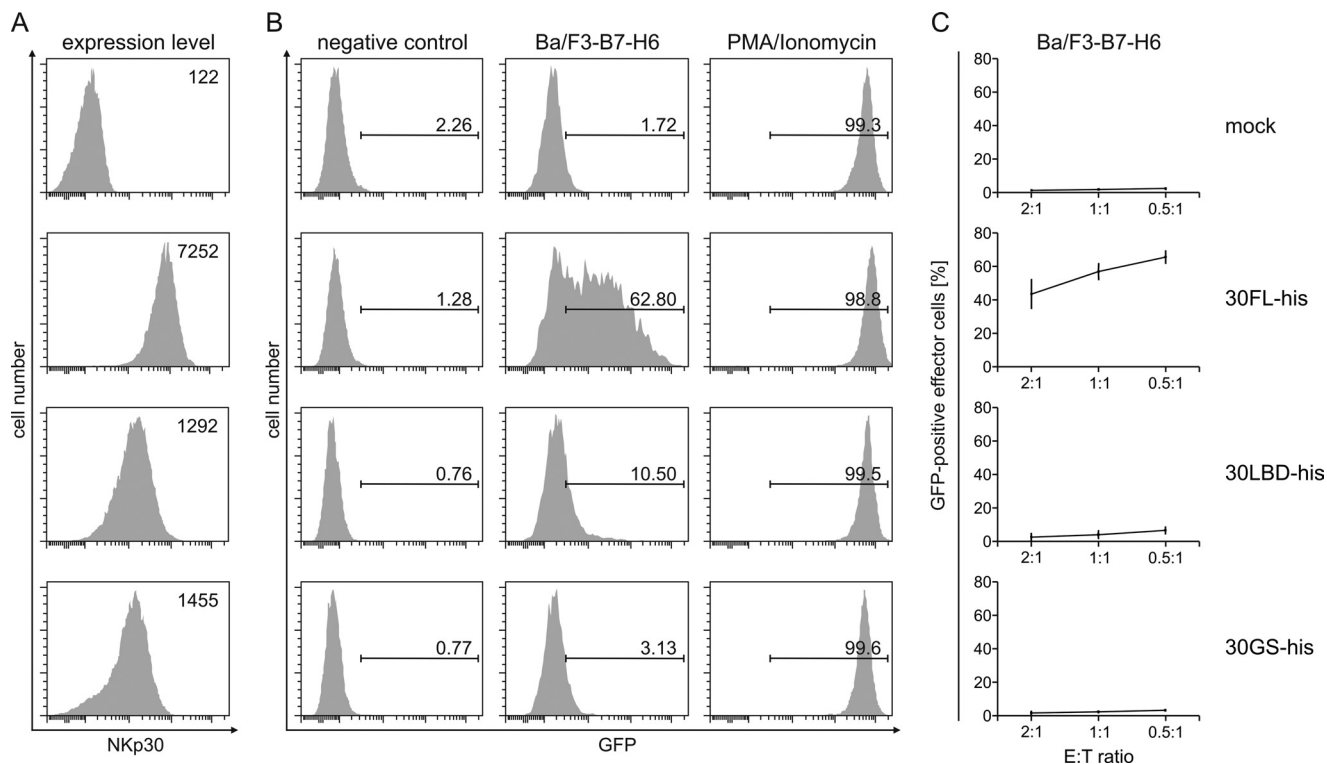
FIGURE 8. **Importance of the stalk domain for NKp30 intracellular signaling.** *A*, A5 reporter cells were retrovirally transduced with 30FL-His (full-length NKp30 with entire ectodomain), 30LBD-His (full-length NKp30 without the stalk), or 30GS-His (full-length NKp30 stalk substituted by GS linker) constructs or a control construct (mock). The indicated A5 transductants were sorted for NKp30 expression, and NKp30 expression levels were determined by staining with an NKp30 antibody. Numbers represent mean fluorescence intensity. *B*, the indicated NKp30 reporter cell lines were mixed with Ba/F3 target cells expressing the NKp30 ligand B7-H6 (Ba/F3-B7-H6) at a 1:1 effector:target ratio or stimulated with PMA and ionomycin. As a negative control, the NKp30 reporter cell lines were incubated without target cells. After 16 h of co-culture, reporter gene expression was determined by analyzing GFP expression in CD4$^+$ A5 cells. *Numbers* in histograms represent the percentage of GFP-positive cells. *C*, the indicated NKp30 reporter cell lines were mixed with Ba/F3 target cells expressing the NKp30 ligand B7-H6 (Ba/F3-B7-H6) at three effector:target (*E:T*) ratios. After 16 h of co-culture, reporter gene expression was determined by analyzing GFP expression in CD4$^+$ A5 cells. Percentages of GFP-positive cells at the indicated reporter cell:target cell ratios are plotted as the average of four independent experiments. *Error bars* represent S.E.

limitation, we generated a novel set of NKp30-Ig fusion proteins with minimal binding affinity to the FcγR. Based on these proteins, we identified the so far neglected stalk domain of NKp30 as an important module of the ectodomain of NKp30 for engagement of cellular ligands. We demonstrated that the integrity of the entire stalk domain with respect to sequence and length is essential for ligand binding and subsequent intracellular signaling. In addition, we showed that *N*-linked glycosylation of the ectodomain of NKp30 impacts the affinity of ligand binding and subsequent CD3ζ signaling as well. Therefore, the glycosylation status of NKp30 might be a way to tune ligand recognition and NKp30-dependent NK cell cytotoxicity.

Productive interaction of an NK cell with a target cell involves the formation of a stable and highly organized immunological synapse bridging an intercellular cleft of roughly 8 nm (as deduced from the length of an NKG2D-MHC I chain-related gene A (MICA) pair) (45, 46). Therefore, we hypothesized that the stalk domain of NKp30 might act as a flexible spacer for the LBD reminiscent of Ly49A (47). Strikingly, substitution of the stalk domain with a flexible length-matched GS linker or C-terminal truncation by only 3 amino acids led to a significant reduction in ligand binding affinity and a loss of CD3ζ signaling. These data demonstrate that the stalk domain contributes directly to ligand binding rather than acting as a spacer for the LBD. This type of contribution is different from that described

previously for the two other NCRs, NKp44 and NKp46. In the case of NKp44, sialic acid moieties attached to the stalk domain of NKp44 bind to influenza hemagglutinin and other viral hemagglutinin-neuraminidase proteins (24, 25, 49). For NKp46, it was shown that the *O*-glycosylated threonine at position 225 within the stalk of this receptor is critical for its binding to viral hemagglutinins (50).

The stalk domain was not resolved in the x-ray crystal structure of an NKp30·B7-H6 complex (30), which indicates flexibility and might argue against a direct contribution of the stalk domain to the B7-H6 binding interface. However, the stalk domain might contribute in a different way to ligand binding when it is connected to the TMD instead of being a "flexible C-terminal tail" of the soluble LBD. The stalk domain is rich in hydrophobic amino acids, which might favor the formation of NKp30 oligomers, leading to increased apparent affinity for the ligand due to increased avidity. Although NK cell killing is not exclusively dependent on NKp30, this idea could at least partially explain the previous observation that some cell lines are killed by NK cells but fail to bind NKp30-Ig proteins devoid of a functional stalk domain (24, 36).

Protein function can be modulated by posttranslational modifications such as glycosylation, which differs among tissues and cell types (51). In this context, we and others could show alterations in ligand binding of NKp30 from different
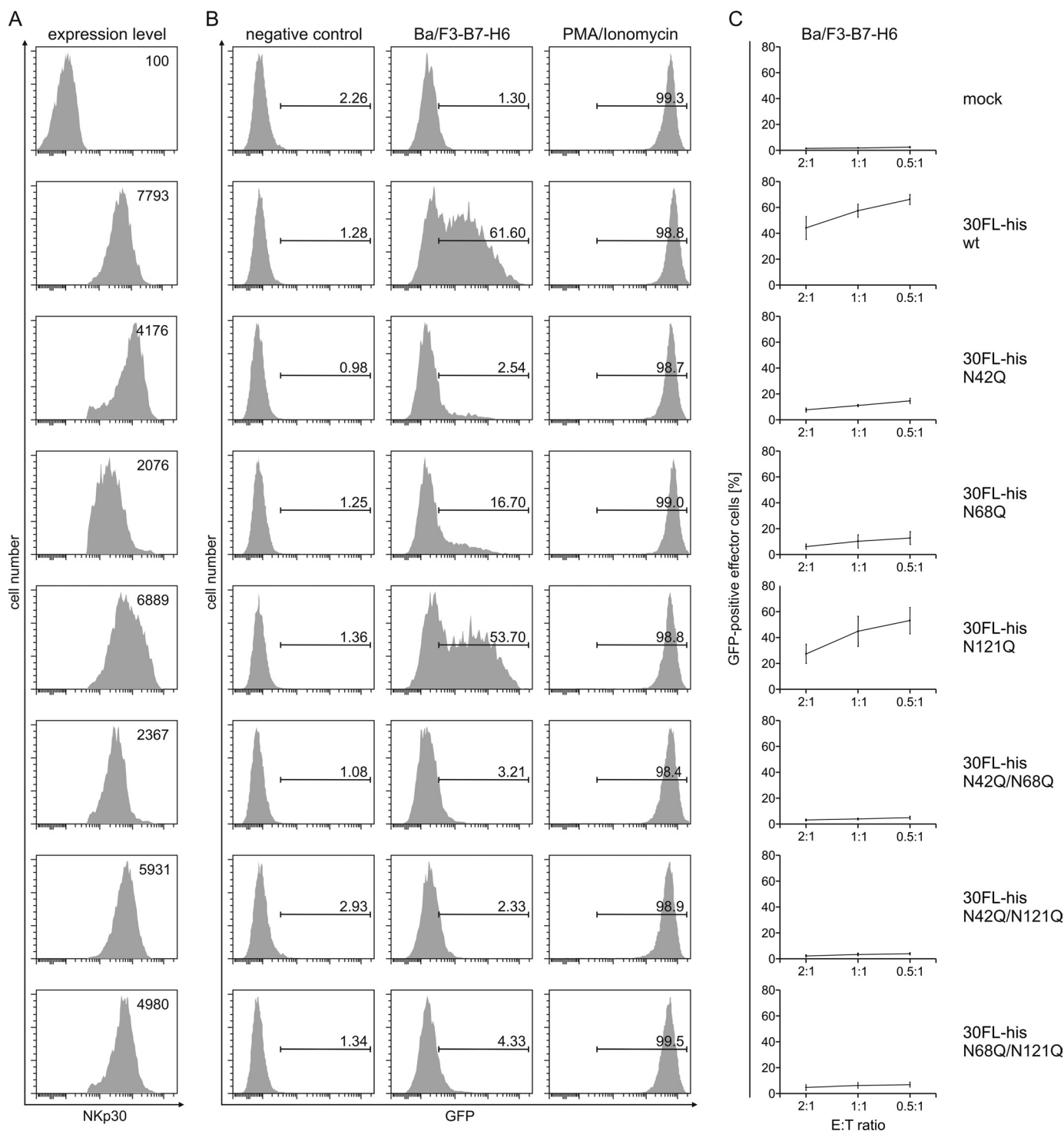
FIGURE 9. **The glycosylation status of NKp30 influences intracellular signaling.** *A*, A5 reporter cells were retrovirally transduced with 30FL-His constructs (WT and three single (N42Q, N68Q, and N121Q) and three double (N42Q/N68Q, N42Q/121Q, and N68Q/N121Q) amino acid mutations) or a control construct (mock). The indicated A5 transductants were sorted for NKp30 expression, and NKp30 expression levels were determined by staining with an NKp30 antibody. *Numbers* represent mean fluorescence intensity. *B*, the indicated NKp30 reporter cell lines were mixed with Ba/F3 target cells expressing the NKp30 ligand B7-H6 (Ba/F3-B7-H6) at a 1:1 effector:target ratio or stimulated with PMA and ionomycin. As a negative control, the NKp30 reporter cell lines were incubated without target cells. After 16 h of co-culture, reporter gene expression was determined by analyzing GFP expression in CD4$^+$ A5 cells. *Numbers* in histograms represent the percentage of GFP-positive cells. *C*, the indicated NKp30 reporter cell lines were mixed with Ba/F3-B7-H6 cells at three effector:target (*E:T*) ratios. After 16 h of co-culture, reporter gene expression was determined by analyzing GFP expression in CD4$^+$ A5 cells. Percentages of GFP-positive cells at the indicated reporter cell:target cell ratios are plotted as the average of four independent experiments. *Error bars* represent S.E.

expression hosts (Ref. 52 and supplemental Fig. S7). These findings are supported by *in vivo* data from the endometrial epithelium demonstrating increased expression of differentially gly-

cosylated variants of NKp30 (53). Along this line, it has already been shown that depending on the NKp30 isoform distinct signals are transmitted (48).

Based on our results, NKp30 is *N*-linked glycosylated at all three consensus motifs within the LBD. Most importantly, these *in vitro* data were confirmed *in vivo* on primary NK cells by a mass spectrometry-based approach (supplemental Fig. S8). Therefore, it is not surprising that the NKp30 variant devoid of all glycosylation targeting sites for *N*-linked glycosylation (N42Q/N68Q/N121Q) was not expressed in our CD3ζ reporter system. Moreover, this result argues for the presence of differentially glycosylated variants of NKp30 in NK cells rather than the existence of functional non-glycosylated variants.

Although the glycosylation acceptor sites are located outside of the B7-H6 binding pocket of NKp30 (30), we showed that differential glycosylation of NKp30 impacts the ligand binding affinity of NKp30 because engagement of NKp30 and B7-H6 was dependent on glycosylation of Asn-42. Moreover, glycosylation of Asn-42 and Asn-68 is essential for efficient intracellular signaling. In the x-ray crystal structure of the NKp30·B7-H6 complex (30), Asn-42 is located at the opposite side of the B7-H6 binding pocket of the LBD. Interestingly, comparison of the unbound (29) and B7-H6-bound structures of NKp30 (30) reveals that Asn-68 is situated underneath the B7-H6 binding pocket within a sequence stretch that undergoes structural rearrangements upon ligand binding. These data suggest that glycosylation of Asn-42 and/or Asn-68 might contribute to subtle conformational changes of NKp30 and therefore shape the ligand binding pocket. Notably, for binding of NKp30 to its cognate ligand BAG-6, glycosylation of Asn-68 was critical, whereas glycosylation at Asn-42 and Asn-121 had less impact. Notably, both available crystal structures of human NKp30 (29, 30) are derived from purified NKp30 protein after heterologous expression in inclusion bodies of *Escherichia coli* and subsequent refolding. Therefore, these NKp30 proteins are not glycosylated. Rearrangement of the binding pocket might be of particular importance in light of the broad spectrum of nonrelated ligands that are recognized by NKp30 when compared with the pool of structurally related ligands of NKG2D. To date, the *in vivo* glycosylation pattern and composition of *N*-linked glycans within NKp30 in the plasma membrane of NK cells is unknown mainly due to limited availability of NK cell-derived homogeneously glycosylated NKp30 and the technically demanding analytic process. Another layer of complexity is given by the observation that NKp30 derived from a polyclonal NK cell population appeared as a broad band (30–45 kDa) in reducing SDS-PAGE (12); this might reflect pools of differentially glycosylated NKp30 on the level of individual cells or the entire population of NK cells. One future perspective to overcome these limitations toward the determination of the native glycosylation pattern of NKp30 might be the use of NKp30-Ig fusion proteins derived from stably transduced NK-92 cells.

REFERENCES

1. Vivier, E., Tomasello, E., Baratin, M., Walzer, T., and Ugolini, S. (2008) Functions of natural killer cells. *Nat. Immunol.* **9,** 503–510
2. Funke, J., Dürr, R., Dietrich, U., and Koch, J. (2011) Natural killer cells in HIV-1 infection: a double-edged sword. *AIDS Rev.* **13,** 67–76
3. Groth, A., Klöss, S., von Strandmann, E. P., Koehl, U., and Koch, J. (2011) Mechanisms of tumor and viral immune escape from natural killer cell-mediated surveillance. *J. Innate Immun.* **3,** 344–354
4. Moretta, A., Marcenaro, E., Parolini, S., Ferlazzo, G., and Moretta, L. (2008) NK cells at the interface between innate and adaptive immunity. *Cell Death Differ.* **15,** 226–233
5. Wehner, R., Dietze, K., Bachmann, M., and Schmitz, M. (2011) The bidirectional crosstalk between human dendritic cells and natural killer cells. *J. Innate Immun.* **3,** 258–263
6. Moretta, A., Bottino, C., Vitale, M., Pende, D., Cantoni, C., Mingari, M. C., Biassoni, R., and Moretta, L. (2001) Activating receptors and coreceptors involved in human natural killer cell-mediated cytolysis. *Annu. Rev. Immunol.* **19,** 197–223
7. Biassoni, R. (2009) Human natural killer receptors, co-receptors, and their ligands. *Curr. Protoc. Immunol.* **Chapter 14,** Unit 14.10
8. Costello, R. T., Sivori, S., Marcenaro, E., Lafage-Pochitaloff, M., Mozziconacci, M. J., Reviron, D., Gastaut, J. A., Pende, D., Olive, D., and Moretta, A. (2002) Defective expression and function of natural killer cell-triggering receptors in patients with acute myeloid leukemia. *Blood* **99,** 3661–3667
9. Srivastava, B. I., and Srivastava, M. D. (2006) Expression of natural cytotoxicity receptors NKp30, NKp44, and NKp46 mRNAs and proteins by human hematopoietic and non-hematopoietic cells. *Leuk. Res.* **30,** 37–46
10. Sivori, S., Parolini, S., Marcenaro, E., Castriconi, R., Pende, D., Millo, R., and Moretta, A. (2000) Involvement of natural cytotoxicity receptors in human natural killer cell-mediated lysis of neuroblastoma and glioblastoma cell lines. *J. Neuroimmunol.* **107,** 220–225
11. Sivori, S., Pende, D., Bottino, C., Marcenaro, E., Pessino, A., Biassoni, R., Moretta, L., and Moretta, A. (1999) NKp46 is the major triggering receptor involved in the natural cytotoxicity of fresh or cultured human NK cells. Correlation between surface density of NKp46 and natural cytotoxicity against autologous, allogeneic or xenogeneic target cells. *Eur. J. Immunol.* **29,** 1656–1666
12. Pende, D., Parolini, S., Pessino, A., Sivori, S., Augugliaro, R., Morelli, L., Marcenaro, E., Accame, L., Malaspina, A., Biassoni, R., Bottino, C., Moretta, L., and Moretta, A. (1999) Identification and molecular characterization of NKp30, a novel triggering receptor involved in natural cytotoxicity mediated by human natural killer cells. *J. Exp. Med.* **190,** 1505–1516
13. Pessino, A., Sivori, S., Bottino, C., Malaspina, A., Morelli, L., Moretta, L., Biassoni, R., and Moretta, A. (1998) Molecular cloning of NKp46: a novel member of the immunoglobulin superfamily involved in triggering of natural cytotoxicity. *J. Exp. Med.* **188,** 953–960
14. Sivori, S., Vitale, M., Morelli, L., Sanseverino, L., Augugliaro, R., Bottino, C., Moretta, L., and Moretta, A. (1997) p46, a novel natural killer cell-specific surface molecule that mediates cell activation. *J. Exp. Med.* **186,** 1129–1136
15. Vitale, M., Bottino, C., Sivori, S., Sanseverino, L., Castriconi, R., Marcenaro, E., Augugliaro, R., Moretta, L., and Moretta, A. (1998) NKp44, a novel triggering surface molecule specifically expressed by activated natural killer cells, is involved in non-major histocompatibility complex-restricted tumor cell lysis. *J. Exp. Med.* **187,** 2065–2072
16. Arnon, T. I., Achdout, H., Levi, O., Markel, G., Saleh, N., Katz, G., Gazit, R., Gonen-Gross, T., Hanna, J., Nahari, E., Porgador, A., Honigman, A., Plachter, B., Mevorach, D., Wolf, D. G., and Mandelboim, O. (2005) Inhibition of the NKp30 activating receptor by pp65 of human cytomegalovirus. *Nat. Immunol.* **6,** 515–523
17. Pogge von Strandmann, E., Simhadri, V. R., von Tresckow, B., Sasse, S., Reiners, K. S., Hansen, H. P., Rothe, A., Böll, B., Simhadri, V. L., Borchmann, P., McKinnon, P. J., Hallek, M., and Engert, A. (2007) Human leukocyte antigen-B-associated transcript 3 is released from tumor cells and engages the NKp30 receptor on natural killer cells. *Immunity* **27,** 965–974
18. Simhadri, V. R., Reiners, K. S., Hansen, H. P., Topolar, D., Simhadri, V. L.,

Nohroudi, K., Kufer, T. A., Engert, A., and Pogge von Strandmann, E. (2008) Dendritic cells release HLA-B-associated transcript-3 positive exosomes to regulate natural killer function. *PLoS One* **3,** e3377

19. Brandt, C. S., Baratin, M., Yi, E. C., Kennedy, J., Gao, Z., Fox, B., Haldeman, B., Ostrander, C. D., Kaifu, T., Chabannon, C., Moretta, A., West, R., Xu, W., Vivier, E., and Levin, S. D. (2009) The B7 family member B7-H6 is a tumor cell ligand for the activating natural killer cell receptor NKp30 in humans. *J. Exp. Med.* **206,** 1495–1503

20. Vitale, M., Della Chiesa, M., Carlomagno, S., Pende, D., Aricò, M., Moretta, L., and Moretta, A. (2005) NK-dependent DC maturation is mediated by TNFα and IFNγ released upon engagement of the NKp30 triggering receptor. *Blood* **106,** 566–571

21. Ferlazzo, G., Tsang, M. L., Moretta, L., Melioli, G., Steinman, R. M., and Münz, C. (2002) Human dendritic cells activate resting natural killer (NK) cells and are recognized via the NKp30 receptor by activated NK cells. *J. Exp. Med.* **195,** 343–351

22. Bloushtain, N., Qimron, U., Bar-Ilan, A., Hershkovitz, O., Gazit, R., Fima, E., Korc, M., Vlodavsky, I., Bovin, N. V., and Porgador, A. (2004) Membrane-associated heparan sulfate proteoglycans are involved in the recognition of cellular targets by NKp30 and NKp46. *J. Immunol.* **173,** 2392–2401

23. Warren, H. S., Jones, A. L., Freeman, C., Bettadapura, J., and Parish, C. R. (2005) Evidence that the cellular ligand for the human NK cell activation receptor NKp30 is not a heparan sulfate glycosaminoglycan. *J. Immunol.* **175,** 207–212

24. Arnon, T. I., Lev, M., Katz, G., Chernobrov, Y., Porgador, A., and Mandelboim, O. (2001) Recognition of viral hemagglutinins by NKp44 but not by NKp30. *Eur. J. Immunol.* **31,** 2680–2689

25. Mandelboim, O., Lieberman, N., Lev, M., Paul, L., Arnon, T. I., Bushkin, Y., Davis, D. M., Strominger, J. L., Yewdell, J. W., and Porgador, A. (2001) Recognition of haemagglutinins on virus-infected cells by NKp46 activates lysis by human NK cells. *Nature* **409,** 1055–1060

26. Draghi, M., Pashine, A., Sanjanwala, B., Gendzekhadze, K., Cantoni, C., Cosman, D., Moretta, A., Valiante, N. M., and Parham, P. (2007) NKp46 and NKG2D recognition of infected dendritic cells is necessary for NK cell activation in the human response to influenza infection. *J. Immunol.* **178,** 2688–2698

27. Jarahian, M., Fiedler, M., Cohnen, A., Djandji, D., Hämmerling, G. J., Gati, C., Cerwenka, A., Turner, P. C., Moyer, R. W., Watzl, C., Hengel, H., and Momburg, F. (2011) Modulation of NKp30- and NKp46-mediated natural killer cell responses by poxviral hemagglutinin. *PLoS Pathog.* **7,** e1002195

28. Rosental, B., Brusilovsky, M., Hadad, U., Oz, D., Appel, M. Y., Afergan, F., Yossef, R., Rosenberg, L. A., Aharoni, A., Cerwenka, A., Campbell, K. S., Braiman, A., and Porgador, A. (2011) Proliferating cell nuclear antigen is a novel inhibitory ligand for the natural cytotoxicity receptor NKp44. *J. Immunol.* **187,** 5693–5702

29. Joyce, M. G., Tran, P., Zhuravleva, M. A., Jaw, J., Colonna, M., and Sun, P. D. (2011) Crystal structure of human natural cytotoxicity receptor NKp30 and identification of its ligand binding site. *Proc. Natl. Acad. Sci. U.S.A.* **108,** 6223–6228

30. Li, Y., Wang, Q., and Mariuzza, R. A. (2011) Structure of the human activating natural cytotoxicity receptor NKp30 bound to its tumor cell ligand B7-H6. *J. Exp. Med.* **208,** 703–714

31. Johnson, J. P., Demmer-Dieckmann, M., Meo, T., Hadam, M. R., and Riethmüller, G. (1981) Surface antigens of human melanoma cells defined by monoclonal antibodies. I. Biochemical characterization of two antigens found on cell lines and fresh tumors of diverse tissue origin. *Eur. J. Immunol.* **11,** 825–831

32. Andersen, P. S., Menné, C., Mariuzza, R. A., Geisler, C., and Karjalainen, K. (2001) A response calculus for immobilized T cell receptor ligands. *J. Biol. Chem.* **276,** 49125–49132

33. Anliker, B., Abel, T., Kneissl, S., Hlavaty, J., Caputi, A., Brynza, J., Schneider, I. C., Münch, R. C., Petznek, H., Kontermann, R. E., Koehl, U., Johnston, I. C., Keinänen, K., Müller, U. C., Hohenadl, C., Monyer, H., Cichutek, K., and Buchholz, C. J. (2010) Specific gene transfer to neurons, endothelial cells and hematopoietic progenitors with lentiviral vectors. *Nat. Methods* **7,** 929–935

34. Weber, K., Bartsch, U., Stocking, C., and Fehse, B. (2008) A multicolor panel of novel lentiviral "gene ontology" (LeGO) vectors for functional gene analysis. *Mol. Ther.* **16,** 698–706

35. Fiering, S., Northrop, J. P., Nolan, G. P., Mattila, P. S., Crabtree, G. R., and Herzenberg, L. A. (1990) Single cell assay of a transcription factor reveals a threshold in transcription activated by signals emanating from the T-cell antigen receptor. *Genes Dev.* **4,** 1823–1834

36. Mandelboim, O., Malik, P., Davis, D. M., Jo, C. H., Boyson, J. E., and Strominger, J. L. (1999) Human CD16 as a lysis receptor mediating direct natural killer cell cytotoxicity. *Proc. Natl. Acad. Sci. U.S.A.* **96,** 5640–5644

37. Duncan, A. R., Woof, J. M., Partridge, L. J., Burton, D. R., and Winter, G. (1988) Localization of the binding site for the human high-affinity Fc receptor on IgG. *Nature* **332,** 563–564

38. Schroeder, H. W., Jr., and Cavacini, L. (2010) Structure and function of immunoglobulins. *J. Allergy Clin. Immunol.* **125,** S41–52

39. Zheng, X. X., Steele, A. W., Hancock, W. W., Kawamoto, K., Li, X. C., Nickerson, P. W., Li, Y., Tian, Y., and Strom, T. B. (1999) IL-2 receptor-targeted cytolytic IL-2/Fc fusion protein treatment blocks diabetogenic autoimmunity in nonobese diabetic mice. *J. Immunol.* **163,** 4041–4048

40. Duncan, A. R., and Winter, G. (1988) The binding site for C1q on IgG. *Nature* **332,** 738–740

41. Byrd, A., Hoffmann, S. C., Jarahian, M., Momburg, F., and Watzl, C. (2007) Expression analysis of the ligands for the Natural Killer cell receptors NKp30 and NKp44. *PLoS One* **2,** e1339

42. Anderson, C. L. (1982) Isolation of the receptor for IgG from a human monocyte cell line (U937) and from human peripheral blood monocytes. *J. Exp. Med.* **156,** 1794–1806

43. McCool, D., Birshtein, B. K., and Painter, R. H. (1985) Structural requirements of immunoglobulin G for binding to the Fc gamma receptors of the human tumor cell lines U937, HL-60, ML-1, and K562. *J. Immunol.* **135,** 1975–1980

44. Hofmann, K., and Stoffel, W. (1993) TMbase - A database of membrane spanning protein segments. *Biol. Chem. Hoppe-Seyler* **374,** 166

45. McCann, F. E., Suhling, K., Carlin, L. M., Eleme, K., Taner, S. B., Yanagi, K., Vanherberghen, B., French, P. M., and Davis, D. M. (2002) Imaging immune surveillance by T cells and NK cells. *Immunol. Rev.* **189,** 179–192

46. Orange, J. S. (2008) Formation and function of the lytic NK-cell immunological synapse. *Nat. Rev. Immunol.* **8,** 713–725

47. Doucey, M. A., Scarpellino, L., Zimmer, J., Guillaume, P., Luescher, I. F., Bron, C., and Held, W. (2004) Cis association of Ly49A with MHC class I restricts natural killer cell inhibition. *Nat. Immunol.* **5,** 328–336

48. Delahaye, N. F., Rusakiewicz, S., Martins, I., Ménard, C., Roux, S., Lyonnet, L., Paul, P., Sarabi, M., Chaput, N., Semeraro, M., Minard-Colin, V., Poirier-Colame, V., Chaba, K., Flament, C., Baud, V., Authier, H., Kerdine-Römer, S., Pallardy, M., Cremer, I., Peaudecerf, L., Rocha, B., Valteau-Couanet, D., Gutierrez, J. C., Nunès, J. A., Commo, F., Bonvalot, S., Ibrahim, N., Terrier, P., Opolon, P., Bottino, C., Moretta, A., Tavernier, J., Rihet, P., Coindre, J. M., Blay, J. Y., Isambert, N., Emile, J. F., Vivier, E., Lecesne, A., Kroemer, G., and Zitvogel, L. (2011) Alternatively spliced NKp30 isoforms affect the prognosis of gastrointestinal stromal tumors. *Nat. Med.* **17,** 700–707

49. Jarahian, M., Watzl, C., Fournier, P., Arnold, A., Djandji, D., Zahedi, S., Cerwenka, A., Paschen, A., Schirrmacher, V., and Momburg, F. (2009) Activation of natural killer cells by newcastle disease virus hemagglutinin-neuraminidase. *J. Virol.* **83,** 8108–8121

50. Arnon, T. I., Achdout, H., Lieberman, N., Gazit, R., Gonen-Gross, T., Katz, G., Bar-Ilan, A., Bloushtain, N., Lev, M., Joseph, A., Kedar, E., Porgador, A., and Mandelboim, O. (2004) The mechanisms controlling the recognition of tumor- and virus-infected cells by NKp46. *Blood* **103,** 664–672

51. Rudd, P. M., and Dwek, R. A. (1997) Glycosylation: heterogeneity and the 3D structure of proteins. *Crit. Rev. Biochem. Mol. Biol.* **32,** 1–100

52. Hershkovitz, O., Jarahian, M., Zilka, A., Bar-Ilan, A., Landau, G., Jivov, S., Tekoah, Y., Glicklis, R., Gallagher, J. T., Hoffmann, S. C., Zer, H., Mandelboim, O., Watzl, C., Momburg, F., and Porgador, A. (2008) Altered glycosylation of recombinant NKp30 hampers binding to heparan sulfate: a lesson for the use of recombinant immunoreceptors as an immunological tool. *Glycobiology* **18,** 28–41

53. Ponnampalam, A. P., Gargett, C. E., and Rogers, P. A. (2008) Identification and hormonal regulation of a novel form of NKp30 in human endometrial epithelium. *Eur. J. Immunol.* **38,** 216–226